Electronic Supplementary Material (ESI) for New Journal of Chemistry.

<u>Supplementary Information</u>

Self Assembled Reduced Graphene Oxide-Cerium Oxide Nanocomposite@ Cytochrome *c* Hydrogel as a Solid Electrochemical Reactive Oxygen Species Detection Platform

Vijayesh Kumar [1 †], *Abhay Sachdev* [1,2†*], *Ishita Matai* [1,2*]

[1] CSIR-Central Scientific Instruments Organization (CSIR-CSIO), Chandigarh-160030, India.

[2] Academy of Scientific and Innovative Research (AcSIR-CSIO), Chandigarh, India

[†]Authors contributed equally

* Corresponding authors: A.S: abhay.sachdev@csio.res.in; IM: ishitamatai@csio.res.in

Synthesis of graphene oxide (GO): Improved Hummer's method was used for synthesis of GO. In typical synthesis, 1.5 g of graphite powder and 0.75 g of sodium nitrate were dissolved in 35 mL of concentrated sulphuric acid. The solution was then kept on ice bath till the temperature reached 0 °C. Then, 4.5 g of potassium permanganate was slowly dropped in the above solution while maintaining temperature below 20 °C. In this mixture, 50 mL of warm water (35°C - 40°C) was added and kept for stirring overnight at room temperature. The reaction mixture was then kept on an ice bath and 3 mL of hydrogen peroxide was added slowly to stop the oxidation reaction. The reaction mixture was further left undisturbed at room temperature for 20 h. Finally, the obtained product was washed and centrifuged several times with 5 % (v/v) HCl and DI water to get a final pH of 6-7. The powdered GO obtained was ultrasonicated each time in DI water for further synthesis of nanocomposite.

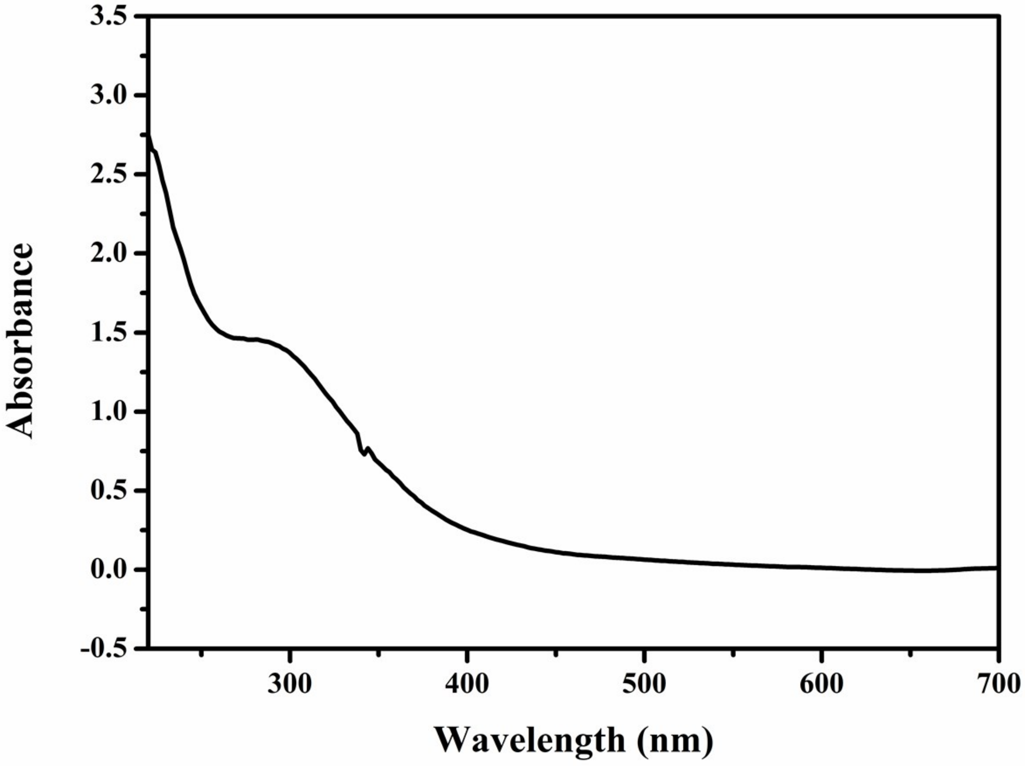

Figure S1. UV-Vis spectra of ·OH radical showing absorption peak at 300 nm.

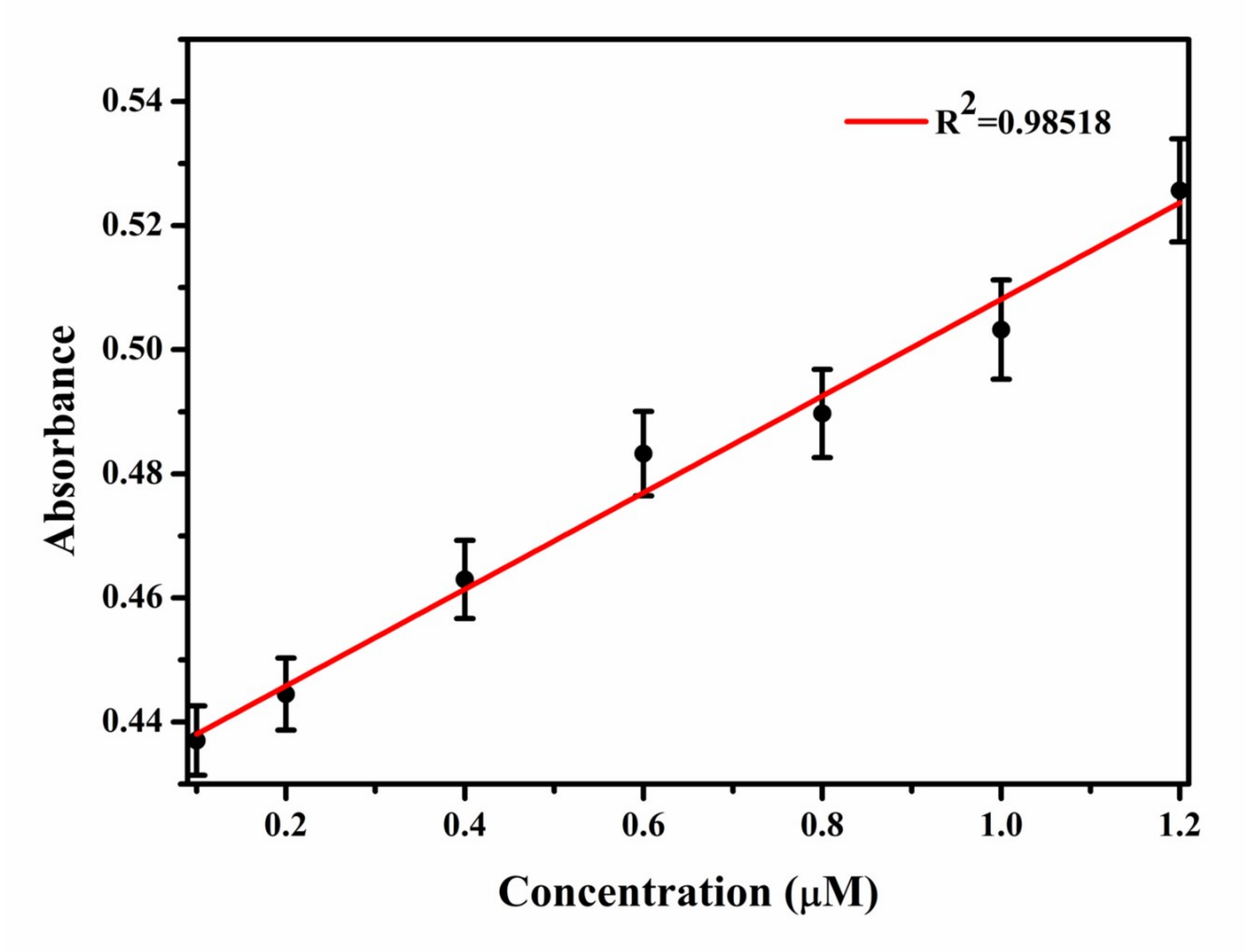

Figure S2. Standard calibration curve for quantification of the ·OH radicals. The linear regression equation: $A=0.078\ C_{\bullet OH} + 0.43$; $R^2= 0.98$.

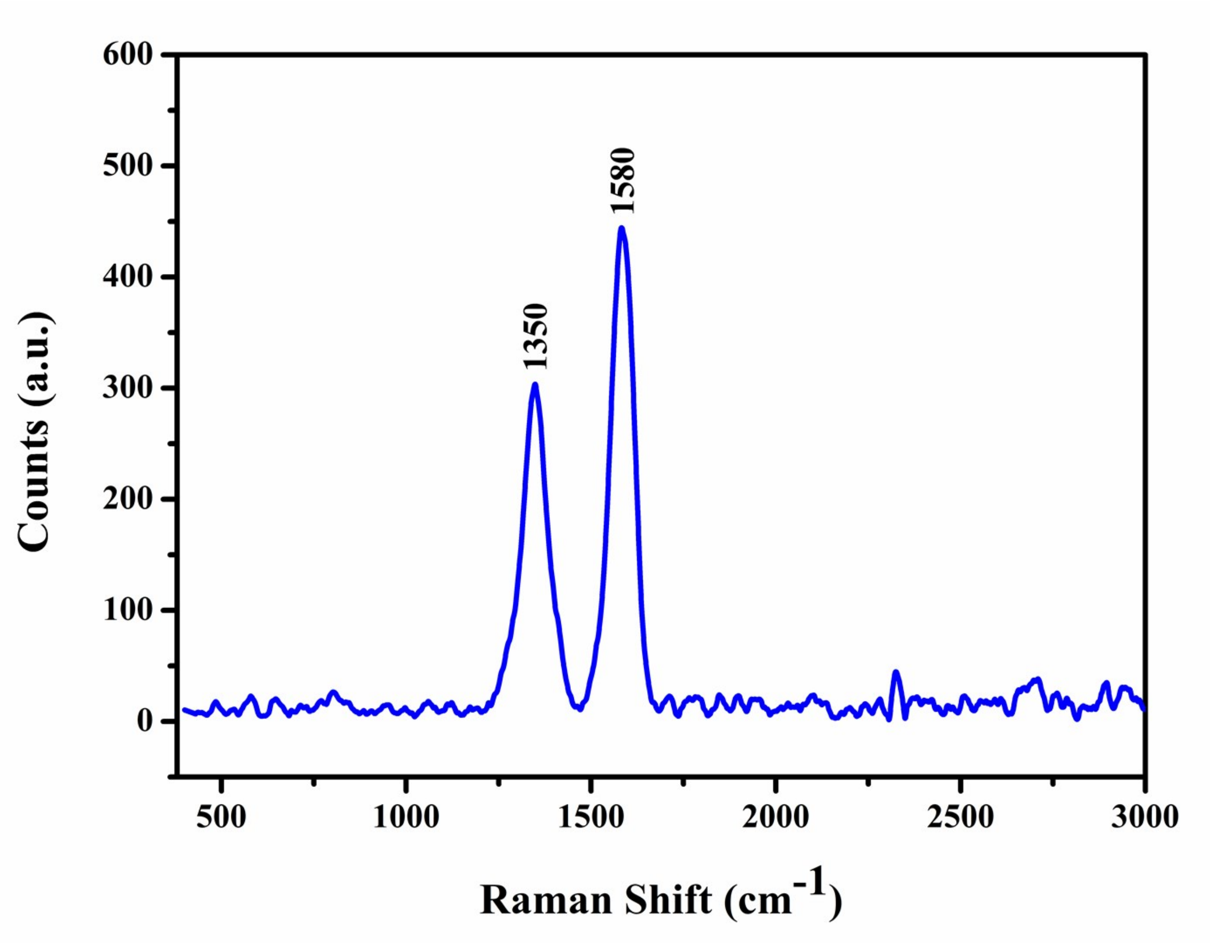

Figure S3. Raman spectra of GO.

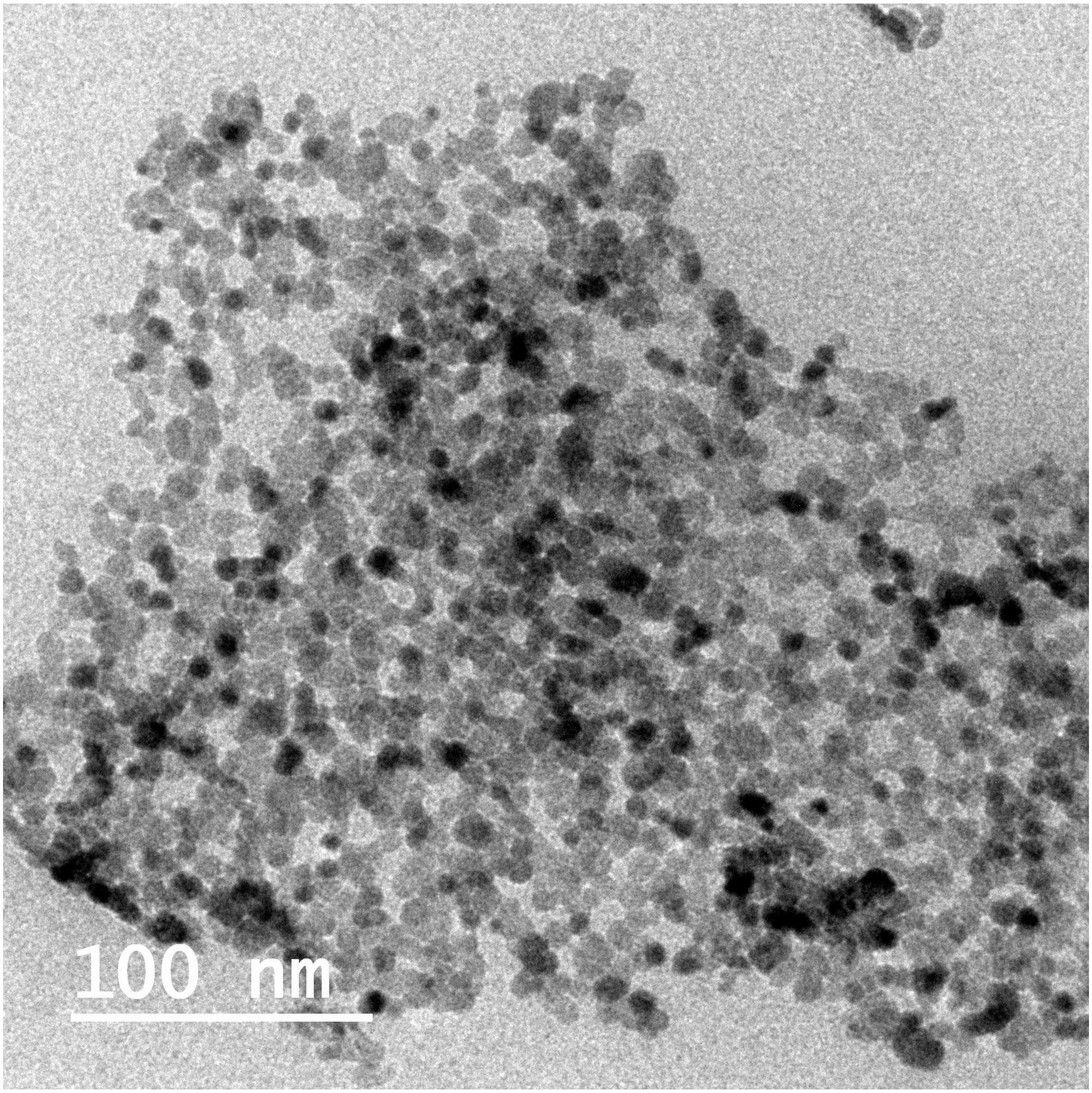

Figure S4. TEM image of rGO-CeO_2 nanocomposite.

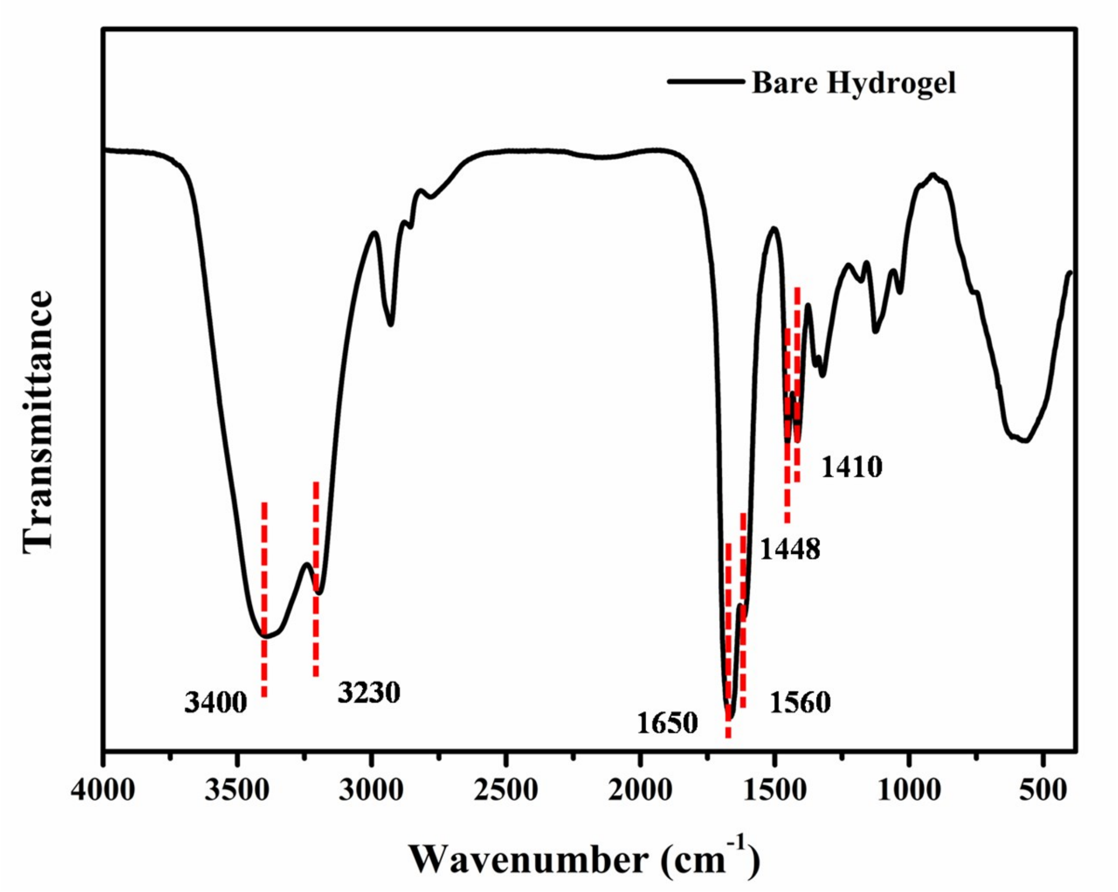

Figure S5. FTIR spectra of the bare hydrogel.

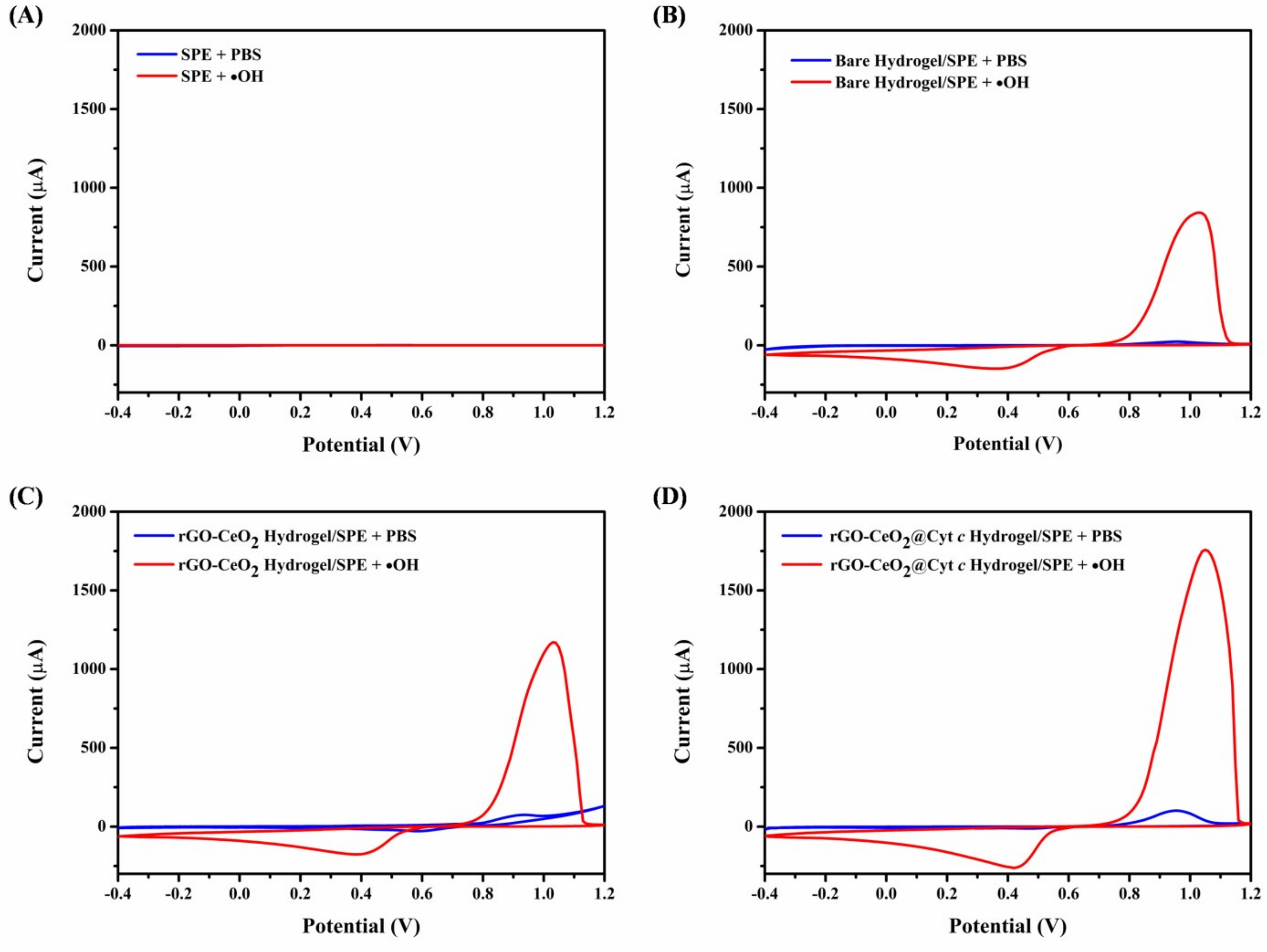

Figure S6. Cyclic voltammograms of different electrodes in the absence (blue curve) and presence (red curve) of 20 μM $^{\bullet}$OH (in 0.1 M PBS, 7.4 pH): (A) SPE, (B) bare hydrogel/SPE, (C) rGO-CeO_2 hydrogel/SPE and (D) rGO-CeO_2@Cyt *c* hydrogel/SPE, at 50 mV s^{-1}.

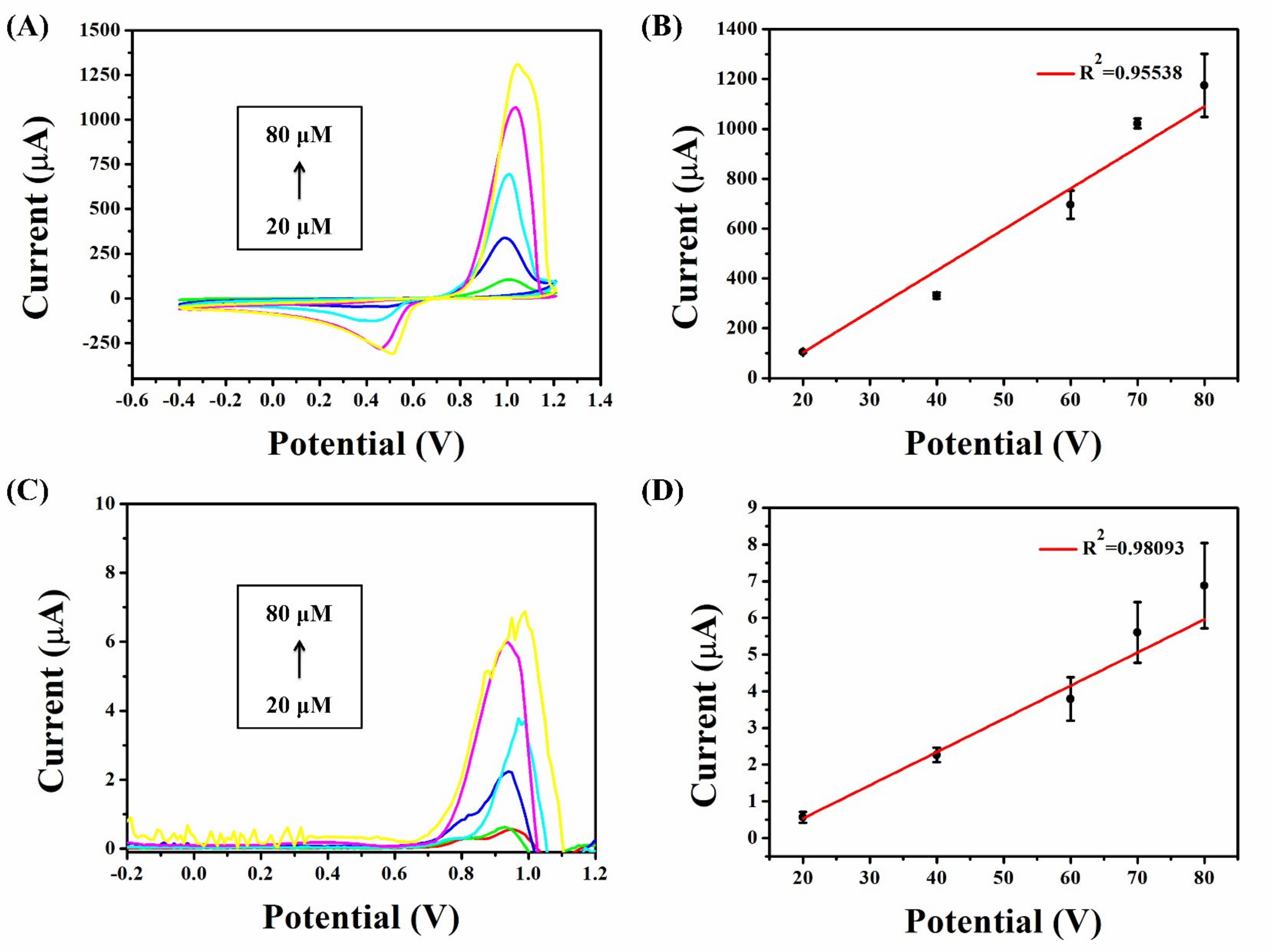

Figure S7. (A) CV and (C) DPV curves for rGO-CeO$_2$@Cyt *c* hydrogel/SPE in the presence of various concentrations of $O_2^{\bullet -}$. Representative linear calibration plots of (B) CV [I (μA) = 16.45 $C_{O_2^{\bullet -}}$ (μM) - 226.12] and (D) DPV [I (μA) = 0.090 $C_{O_2^{\bullet -}}$ (μM) - 1.28] depicting an increase in current response as a function of $O_2^{\bullet -}$ concentration in PBS solutions (pH 7.4).

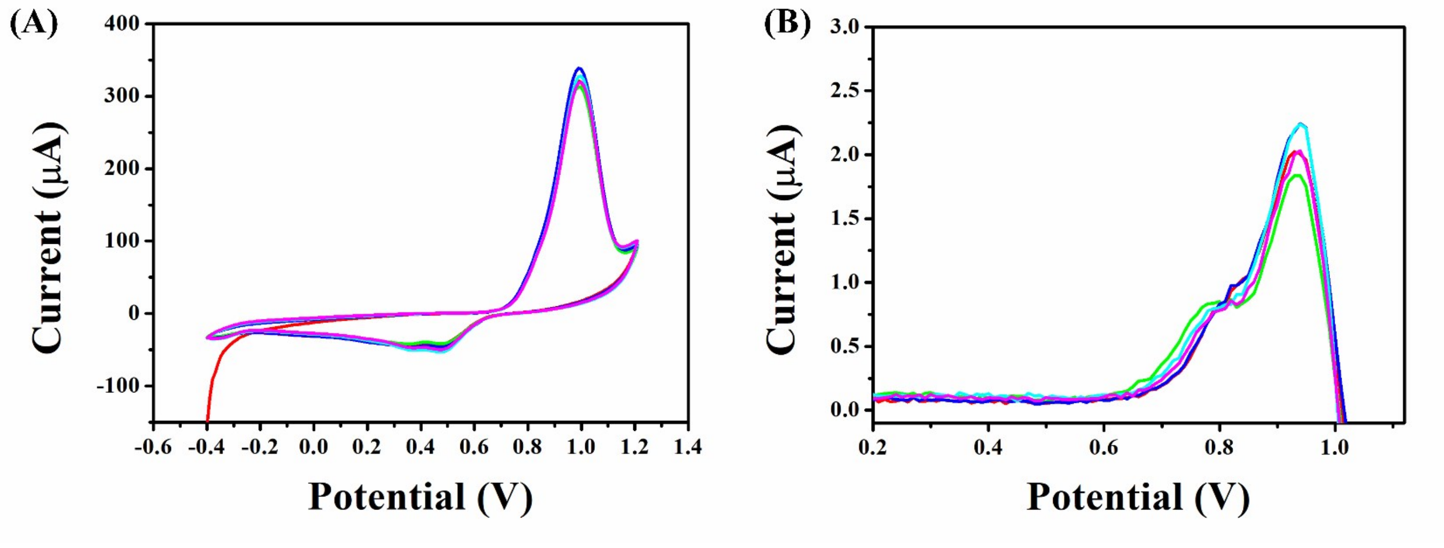

Figure S8. (A) CV and (B) DPV curves showing the detection of $O_2^{\bullet-}$ (40 μM) by rGO-CeO_2@Cyt *c* hydrogel/SPE (n=5) under similar conditions.